



IEEE
NPSS
NUCLEAR & PLASMA
SCIENCES SOCIETY

2025 IEEE NSS MIC RTSD

1 - 8 NOVEMBER 2025, YOKOHAMA, JAPAN

Login



Abstract submission



Submit your abstract here!

Online Program

More information here!

Registration



Start here your registration!

Booth Registration



Get your booth here!



Dear Colleagues,

We are pleased to inform you that the first onsite and hybrid **IEEE Nuclear Science Symposium, Medical Imaging Conference, and Room Temperature Semiconductor Detectors Symposium** in Japan will be held in Yokohama in November 2025. As you may know, Japan is a cluster of small islands in the east Asia, which is isolated from other Asian countries by the sea. Therefore, there are many unique cultural aspects of Japan to enjoy.

The natural beauty of Japan is rich, and magnificent. Mt. Fuji can be seen from Yokohama and Tokyo on sunny days. The Hakone hot spring area is close to Yokohama, where you can enjoy an excellent view of Mt. Fuji and explore the natural hot springs in this area. Kamakura is about 30 minutes by train from Yokohama, where you can enjoy historic wooden buildings and Japanese gardens. Their unique features and harmonies reflect the cultural atmosphere of Japan and the spirit of Japanese fine arts. The choice of a site and dates for an IEEE NSS/MIC/RTSD in Yokohama has a long history.

News

Online Program released

August 4, 2025

[more information here](#)

Presentation Guidelines released

July 16, 2025

[more information here](#)

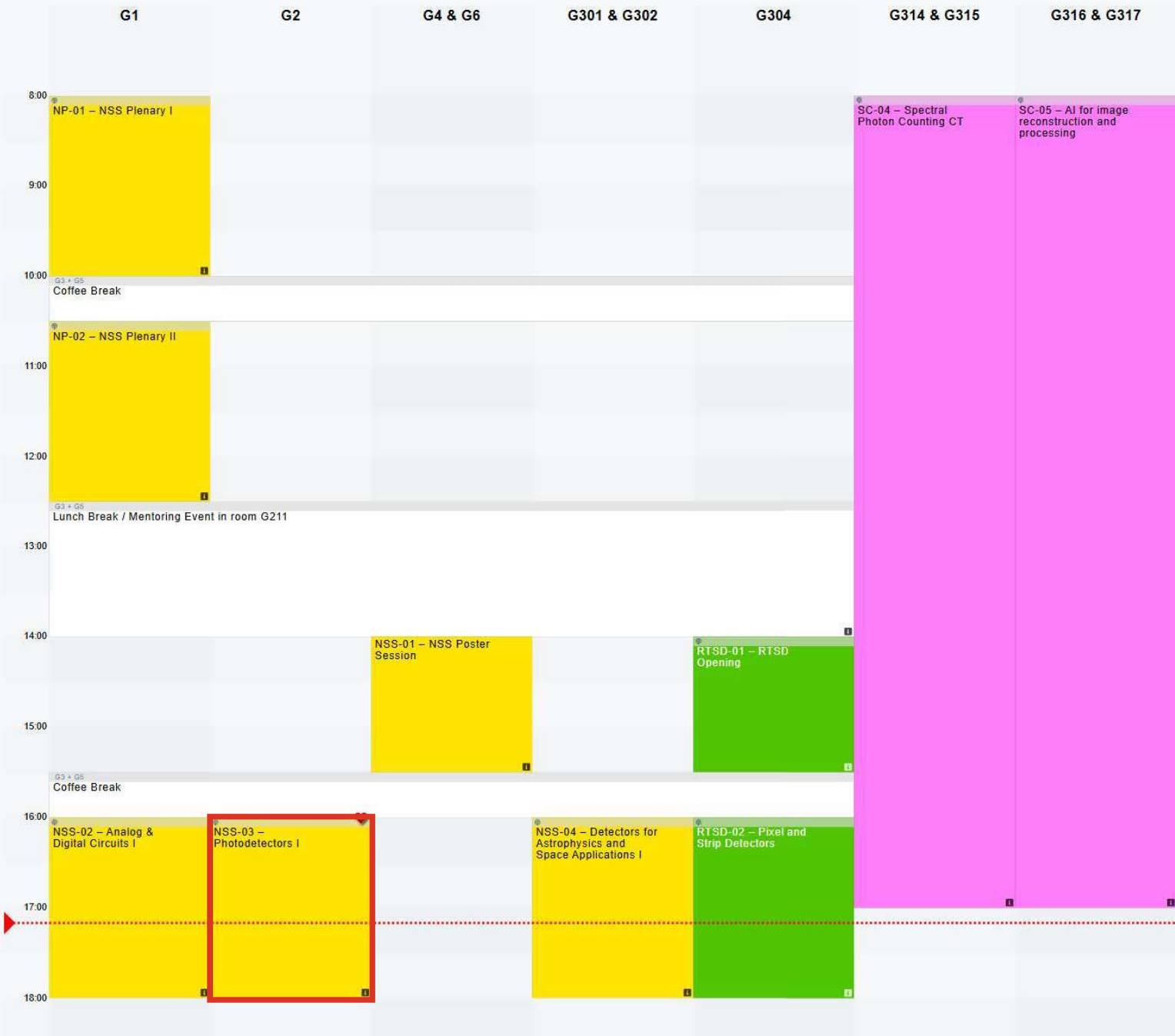
Total overview

Sat, 01 Nov, Sun, 02 Nov, **Mon, 03 Nov**, Tue, 04 Nov, Wed, 05 Nov, Thu, 06 Nov, Fri, 07 Nov, Sat, 08 Nov

Filter tracks: in my schedule Short Courses NSS Session RTSD Session

Please use your mouse/scroll wheel to pan and zoom in the schedule.
Click to open a session.

Reset zoom





Photodetectors I

Session chair: **Fabrice Retiere** (TRIUMF, Vancouver, Canada); **Stefan Gundacker** (RWTH Aachen, Aachen, Germany)

Shortcut: **NSS-03**

Date: **Monday, 3 November, 2025, 16:00 - 18:00**

Location: **G2**

Session type: **NSS Session**

Contents

Click on a contribution to preview the abstract content.

The underlined authors are the presenters. The **authors in bold** are the main authors.

16:00	NSS-03-01	Enhanced Photon Counting in PCCT Using EQR SiPM with Pulse Shaping and Pile Up Recovery (#1174)	Contact author individually
		<u>Y. Yan</u> ¹ , L. Zhang ¹ , T. Yuan ¹ , K. Liang ¹ , R. Yang ¹ , T. Sun ¹ , D. Han ¹	
16:15	NSS-03-02	The new NUV-BSI SiPM technology optimized for detection efficiency and radiation tolerance. (#3156)	Contact author individually
		A. Gola ¹ , F. Acerbi ¹ , P. Antonioli ² , F. Caso ¹ , S. Cherry ³ , D. O. Elgewaily ¹ , A. Ficorella ¹ , P. Khachru ¹ , L. Parellada Monreal ¹ , E. Montagna ² , A. Montanari ² , S.I. Kwon ³ , R. Nania ² , G. Paternoster ¹ , R. Preghenella ² , L. Rignanese ² , E. Rovati ² , N. Tosi ²	
16:30	NSS-03-03	Back-Illuminated Single-Photon Avalanche Diode Optimized for Scintillation Detectors (#2151)	Contact author individually
		S. Yook ¹ , H.-S. Choi ^{1,2} , J.D. Song ² , W.-Y. Choi ¹ , M.-J. Lee ¹	
		¹ Yonsei University, Electrical and Electronic Engineering, Seoul, Republic of Korea ² Korea Institute of Science and Technology, Post-Silicon Semiconductor Institute, Seoul, Republic of Korea	
		Abstract Single-photon avalanche diodes (SPADs) are semiconductor photodetectors for next-generation scintillation detectors, which are highly beneficial for many biomedical applications such as fluorescence lifetime imaging microscopy (FLIM), X-ray imaging, and time-of-flight positron emission tomography (ToF-PET). Those applications generally require SPADs with high fill factors and strong sensitivities in the blue-green wavelength range, matching the emission spectrum of commonly used scintillators. While front-illuminated (FI) SPADs are advantageous for detecting blue-green wavelengths due to their shallow junction depth, they suffer from optical losses caused by stacked dielectric layers and low fill factors due to the peripheral region for the guard ring and anode/cathode. These can be addressed using back-illuminated (BI) SPADs, but those devices typically have deeper junctions and smaller pixel pitches, limiting blue-green sensitivity and suitability for biomedical applications. This study presents the optimized BI SPAD with aggressive backside thinning, active-area enlargement, and backside patterning. These structural optimizations reduce the epitaxial thickness, increase photon interaction volume, and enhance internal light scattering, leading to significantly improved photon detection probability (PDP) in the blue-green wavelength range. Experimental results exhibit a PDP increase rate of over 98.21% at 3 V excess bias voltage with a low dark count rate of less than 10 cps/ μm^2 . This work demonstrates a viable BI SPAD for scintillation detectors, especially for biomedical imaging systems requiring large pixel pitches and high blue-green sensitivity.	
		Acknowledgment This work was supported by the Yonsei University Research Fund of 2024(2024-22-0504) and the Challengeable Future Defense Technology R&D Program through the ADD funded by the DAPA(915059201).	
		References [1] Braga, L. H. C., et al. 2014, 'A fully digital 8x16 SiPM array for PET applications with per-pixel TDCs and real-time energy output', <i>IEEE Journal of Solid-State Circuits</i> , vol. 49, no. 1, pp. 301-314, New York: IEEE [2] Du, J., et al. 2016, 'Characterization of large-area SiPM array for PET applications', <i>IEEE Transactions on Nuclear Science</i> , vol. 63, no. 1, pp. 8-16, New York: IEEE [3] Meng, K., et al. 2023, 'High-speed real-time X-ray image recognition based on a pixelated SiPM-coupled scintillator detector with radiation photoelectric neural network structure', <i>IEEE Transactions on Nuclear Science</i> , vol. 70, no. 5, pp. 859-866, New York: IEEE [4] Ha, W.-Y., et al. 2023, 'Single-photon avalanche diode fabricated in standard 55 nm bipolar-CMOS-DMOS technology with sub-20 V breakdown voltage', <i>Optics Express</i> , vol. 31, no. 9, pp. 13798-13805, Washington, DC: Optica Publishing Group [5] Ha, W.-Y., et al. 2024, 'SPAD developed in 55 nm bipolar-CMOS-DMOS technology achieving near 90% PDP', <i>IEEE Journal of Selected Topics in Quantum Electronics</i> , vol. 30, no. 1, pp. 1-10, New York: IEEE [6] Park, E., et al. 2024, 'A back-illuminated SPAD fabricated with 40 nm CMOS image sensor technology achieving near 40% PDP at 940 nm', <i>IEEE Journal of Selected Topics in Quantum Electronics</i> , vol. 30, no. 1, pp. 1-7, New York: IEEE	
		Keywords: Avalanche photodiode (APD), Back-illuminated single-photon avalanche diode (SPAD), Scintillator, Scintillation detector, Photodetector	
		Add question/comment	Check for new question/comment
no questions/comments available			
16:45	NSS-03-04	Advanced Technologies to Reduce Photon Loss and Carrier Recombination for Next-generation SiPM (#1939)	Contact author individually
		<u>Y. Tao</u> ¹ , A. Erickson ¹	
17:00	NSS-03-05	Optical Characterization of Low-Gain Avalanche Diodes (#1815)	Contact author individually
		T. Tsang ¹ , M. Boukchicha ¹ , G. Giacomini ¹ , <u>F. Capocasa</u> ¹	
17:15	NSS-03-06	Pixel and Transmission Line Readouts in Capacitive-Coupled HRPPD MCP-PMTs for High-Precision Timing (#1778)	Contact author individually
		Z. Zobundzija ¹ , V. Sharyy ^{1,5} , D. Yvon ^{1,5} , A. Lyashenko ² , M.A. Popecki ² , M.J. Minot ² , J. Maalmi ³ , D. Breton ³ , C. Morel ⁴ , M. Dupont ⁴	
17:30	NSS-03-07	Timing Resolution of Particle Counting Detectors with Microchannel Plates (#3413)	Contact author individually
		A. S. Tremisín ¹ , O. H. Siegmund ¹ , J. V. Vallerga ¹ , J. B. McPhate ¹ , T. Curtis ¹ , D. T. Tercero ¹ , M. R. Dexter ¹ , R. R. Raffanti ² , S. Roy ³ , S. Morley ³ , A. Us Saleheen ³	
17:45	NSS-03-08	CT-Based Modeling and Experimental Study of Hamamatsu R6233 PMT Non-Uniformity (#3057)	Contact author individually
		<u>G. Ma</u> ¹ , Z. Yuan ²	

Back-Illuminated Single-Photon Avalanche Diode Optimized for Scintillation Detectors

Seyoung Yook, Hyun-Seung Choi, Jin Dong Song, Woo-Young Choi, and Myung-Jae Lee, *Member, IEEE*

Abstract—Single-photon avalanche diodes (SPADs) are semiconductor photodetectors for next-generation scintillation detectors, which are highly beneficial for many biomedical applications such as fluorescence lifetime imaging microscopy (FLIM), X-ray imaging, and time-of-flight positron emission tomography (ToF-PET). Those applications generally require SPADs with high fill factor and strong sensitivities in the blue-green wavelength range, matching the emission spectrum of commonly used scintillators. While front-illuminated (FI) SPADs are advantageous for detecting blue-green wavelengths due to their shallow junction depth, they suffer from optical losses caused by stacked dielectric layers and low fill factor due to the peripheral region for the guard ring and anode/cathode. These can be addressed using back-illuminated (BI) SPADs, but those devices typically have deeper junctions and smaller pixel pitches, limiting blue-green sensitivity and suitability for biomedical applications. This study presents the optimized BI SPAD with aggressive backside thinning, active-area enlargement, and backside patterning. These structural optimizations reduce the epitaxial thickness, increase photon interaction volume, and enhance internal light scattering, leading to significantly improved photon detection probability (PDP) in the blue-green wavelength range. Experimental results exhibit a PDP increase rate of over 98.21% at 3 V excess bias voltage with a low dark count rate of less than 10 cps/ μm^2 . This work demonstrates a viable BI SPAD for scintillation detectors, especially for biomedical imaging systems requiring large pixel pitches and high blue-green sensitivity.

Index Terms—Avalanche photodiode (APD), back-illuminated single-photon avalanche diode (SPAD), scintillator, scintillation detector, photodetector.

I. INTRODUCTION

Single-photon avalanche diodes (SPADs) exhibit exceptional photon sensitivity, enabling the detection of even individual photons. Due to this outstanding capability, SPADs have emerged as a promising solution for biomedical and quantum applications, as well as for light detection and ranging (LiDAR). In particular, scintillation detectors such as X-ray imaging and time-of-flight positron emission tomography (ToF-PET) require SPAD array with high fill factor and sensitivity in the blue-green spectral range, as scintillators used in biomedical applications typically emit photons within this range [1-3]. In the scintillation detector, the scintillator converts high-energy radiation, such as X-ray or gamma ray, into visible photons, and they can be efficiently detected by SPAD array for imaging or timing applications. As shown in Fig. 1, SPADs can be categorized by their illumination direction into front-illuminated (FI) and back-

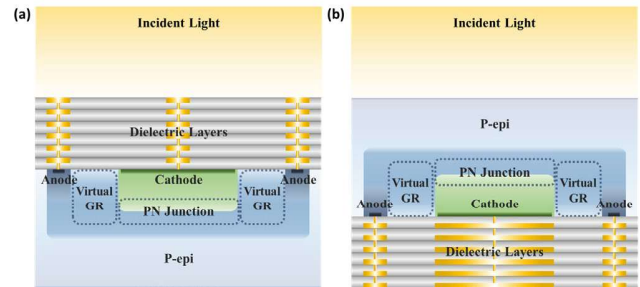


Fig. 1. Cross-sections of (a) FI SPAD and (b) BI SPAD.

illuminated (BI) types. FI SPADs are generally applied for scintillation detectors due to their shallow junction depth, which is advantageous for detecting the blue-green wavelength range [4].

However, dielectric layers stacked on the optical window of FI SPADs result in optical loss [5]. Moreover, the photon detection efficiency of silicon photomultipliers (SiPMs) is limited by the low fill factor of the FI SPAD array. Although microlenses are commonly applied to SPADs to compensate for low fill factor, microlenses are ineffective for scintillator-emitted photons, which typically have wide angular distributions.

These limitations can be addressed through BI SPADs. Since the dielectric layers are stacked under the SPADs' active region, BI SPADs improve optical transmission and enable higher fill factor through 3D stacking. Despite these advantages, BI SPADs also have limitations for applied scintillation detection systems, as BI SPADs exhibit lower blue-green wavelength sensitivity than FI SPADs due to the deeper junction depth and small pixel pitch, which are optimized for LiDAR [6]. In contrast, biomedical imaging systems generally require pixel pitches exceeding 10 μm .

In this study, we demonstrate the structural optimization strategies of BI SPADs for scintillation detectors with enhanced blue-green sensitivity and size scaling.

II. DEVICE STRUCTURE

The cross-sections of the fabricated BI SPADs using a 90 nm CMOS image sensor (CIS) process are shown in Fig. 2. As shown in Fig. 2(a), the default BI SPAD is circular with an active area of 5 μm , a virtual guard-ring width of 2 μm , and an anode width of 1 μm . The deep junction structure based on N-well and deep P-well is adopted for high efficiency of blue-

Manuscript received on May 08, 2025

This work was supported by the Yonsei University Research Fund of 2024(2024-22-0504) and the Challengeable Future Defense Technology R&D Program through the ADD funded by the DAPA(915059201).

The authors are with the Department of Electrical and Electronic Engineering, Yonsei University, Seoul, 03722, Republic of Korea (Corresponding author: Myung-Jae Lee, e-mail: mj.lee@yonsei.ac.kr)

green wavelength in BI SPAD. Additionally, the virtual guard ring with sufficient width is applied to prevent premature edge breakdown in the deep junction structure. Three key structural optimization strategies were introduced to optimize BI SPAD for scintillation detectors: aggressive backside thinning, enlargement of the SPAD's active area, and backside patterning.

First, aggressive backside thinning reduces the epitaxial layer thickness from 5 μm to 3.3 μm . This reduction aligns the junction depth better with the penetration depth of the blue-green wavelength range, consequently enabling sensitivity improvement. Second, the active-area diameter was enlarged from 5 μm to 10 μm , which not only expands the depletion region and lateral diffusion contribution area but also increases the pixel pitch and the fill factor, from approximately 21% to 39%. Lastly, the cross-shape patterns are implemented on the backside silicon surface to induce light scattering, effectively extending the optical path within the device and increasing the probability of photon absorption and detection.

The combined optimizations are applied to the default BI SPAD, and the cross-section of the optimized BI SPAD is depicted in Fig. 2(b). The optimizations result in a remarkable photon sensitivity increase, especially in the blue-green range, with an expanded pixel pitch.

III. MEASUREMENT RESULTS

The performance of the BI SPADs was evaluated through various measurements, including I-V measurement, dark count rate (DCR), light emission test (LET), and photon detection probability (PDP).

In the I-V characteristics, measured under both light and dark conditions, both BI SPADs maintain low dark currents, remaining below 10 pA, and exhibit the same breakdown voltage of about 30.6 V. The normalized DCR values of both devices remain below 10 cps/ μm^2 at the excess bias voltage of 3 V, indicating that noise performance is unaffected by the optimization process. LET results confirm uniform avalanche multiplication across the entire active region, without premature edge breakdown, thanks to the sufficient guard ring width.

PDP is defined as the ratio of detected photons to the number of incident photons on the SPAD's active area, as a function of wavelength. As shown in Fig. 3, PDP measurements were conducted from 400 nm to 600 nm at 25 nm intervals under excess bias voltages of 1, 2, and 3 V. This range corresponds to the emission spectra of typical scintillators used in biomedical imaging, such as LYSO, LSO, and BGO.

According to optimization, the PDP characteristics exhibit significant improvement of more than 98.21 % across the blue-green wavelength under the excess bias voltage of 3 V. The optimized BI SPAD achieves the peak PDP of 55.71 % in the 525 nm wavelength at the excess bias voltage of 3 V, compared to 12.14% for the default BI SPAD under identical conditions.

Comprehensive measurement results confirm that the proposed structural optimization process dramatically enhanced BI SPAD's blue-green wavelength sensitivity while maintaining stable noise performance.

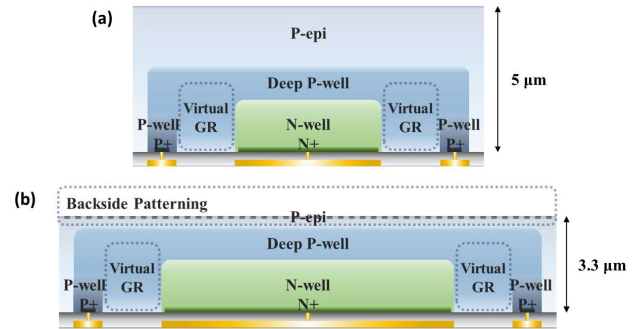


Fig. 2. Cross-sections of (a) default BI SPAD and (b) BI SPAD with backside thinning, active-area enlargement, and backside patterning.

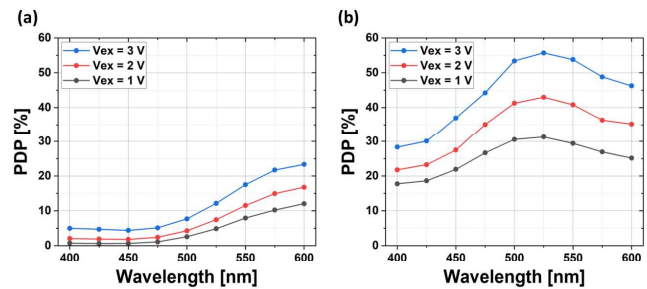


Fig. 3. The PDP characteristics of (a) default BI SPAD and (b) BI SPAD with backside thinning, active-area enlargement, and backside patterning.

IV. CONCLUSION

In conclusion, the BI SPAD is optimized for scintillation detectors with aggressive backside thinning, active-area enlargement, and backside patterning, resulting in significant improvements in blue-green sensitivity, without noise-performance degradation. The proposed innovations not only improve the PDP in the blue-green wavelength range but also address the challenges associated with large pixel pitches and high fill factor, which are key requirements in scintillation detectors.

REFERENCES

- [1] L. H. C. Braga *et al.*, "A fully digital 8×16 SiPM array for PET applications with per-pixel TDCs and real-time energy output," *IEEE J. Solid-State Circuits*, vol. 49, no. 1, pp. 301-314, Jan. 2014, 10.1109/JSSC.2013.2284351.
- [2] J. Du *et al.*, "Characterization of large-area SiPM array for PET applications," *IEEE Trans. Nucl. Sci.*, vol. 63, no. 1, pp. 8-16, Feb. 2016, 10.1109/TNS.2015.2499726.
- [3] K. Meng *et al.*, "High-speed real-time X-ray image recognition based on a pixelated SiPM-coupled scintillator detector with radiation photoelectric neural network structure," *IEEE Trans. Nucl. Sci.*, vol. 70, no. 5, pp. 859-866, May 2023, 10.1109/TNS.2023.3267262.
- [4] W.-Y. Ha *et al.*, "Single-photon avalanche diode fabricated in standard 55 nm bipolar-CMOS-DMOS technology with sub-20 V breakdown voltage," *Opt. Express*, vol. 31, no. 9, pp. 13798-13805, Apr. 2023, 10.1364/OE.485424.
- [5] W.-Y. Ha *et al.*, "SPAD developed in 55 nm bipolar-CMOS-DMOS technology achieving near 90% peak PDP," *IEEE J. Sel. Top. Quantum Electron.*, vol. 30, no. 1, pp. 1-10, Jan.-Feb. 2024, 10.1109/JSTQE.2023.3303678.
- [6] E. Park *et al.*, "A back-illuminated SPAD fabricated with 40 nm CMOS image sensor technology achieving near 40% PDP at 940 nm," *IEEE J. Sel. Top. Quantum Electron.*, vol. 30, no. 1, pp. 1-7, Jan.-Feb. 2024, 10.1109/JSTQE.2023.3272777.